Dynamical Effects of the Dipolar Field Inhomogeneities in High-Resolution NMR: Spectral Clustering and Instabilities

J. Jeener*

Université Libre de Bruxelles (CP-232), B-1050 Brussels, Belgium

(Received 17 August 1998)

In high-resolution NMR in liquids, for "large" nuclear spin magnetization (e.g., water at equilibrium in high field, optically polarized ^{129}Xe, etc.), the interplay of spatial inhomogeneities in the dipolar field with corresponding inhomogeneities in magnetization has unexpected dynamical effects. Starting from equilibrium, the response to a small pulse no longer directly reflects the weak inhomogeneities of external field ("spectral clustering"), and the instabilities which develop after large pulses lead to macroscopically turbulent spin motion. These effects are discussed using various models, and by reference to experimental results of Nacher and co-workers. [S0031-9007(99)08561-0]

PACS numbers: 76.60.Jx, 75.10.Hk, 76.20.+q

In the standard presentation of high-resolution liquid NMR, the observed spectrum is the superposition of the line spectra of the individual molecules, the intermolecular interactions are ignored except as a mechanism contributing to relaxation (and to a small associated line shift), and field inhomogeneities just contribute to the observed linewidth. The present paper shows that, for samples with "large" spin magnetization, the dynamical interplay of inhomogeneities in external field, dipolar field, and spin magnetization can lead to spectral and dynamical behavior very different from traditional expectations.

The pioneering work of Deville *et al.* [1,2] showed that the large equilibrium spin magnetization in solid or liquid ^{3}He generates a classical dipolar field (also called "demagnetizing field") large enough to cause the appearance of strong multiple spin echoes in experiments in which the traditional theory predicts a single echo. Over the last decade, similar effects have been seen in conventional high-resolution NMR on liquid samples containing a high concentration of protons, such as water [3,4]. At room temperature and at a proton NMR frequency of 600 MHz, the equilibrium dipolar field in water (depending upon the shape of the sample) typically shifts the proton NMR frequency by about 1 Hz and linewidths can be less than 0.1 Hz, making the effect very conspicuous. Tipping and precession motion of the spins causes similar motion of the dipolar field. In pulse pair experiments, this mechanism which causes repeated echoes also generates a wealth of additional peaks in 2D spectra, which are very similar to the usual "signature" of multiple quantum coherences. At first, the interpretation of these new features caused some controversy [5,6] which has now been settled by recognizing that predictions in agreement with experiments can be obtained by using the notion of an average classical dipolar field acting on the spins [7–9] (the same predictions can be obtained by alternative techniques).

Recently, other unexpected manifestations of the dipolar field have been observed by Nacher *et al.* [10–12] in their study of dilute solutions of hyperpolarized ^{3}He in ^{4}He at lattice temperatures of the order of 0.2 K. The sample was contained in a capillary tube in the shape of a U, with the constant external magnetic field parallel to the straight arms of the U. With this geometry, the "equilibrium" dipolar field varies continuously from $+2B_d$ in the vertical arms to $-B_d$ at the bottom of the U; hence, one would naively expect an absorption spectrum (i.e., the Fourier transform of the response to a small pulse of transverse magnetic field) with the corresponding continuous shape, resembling a powder pattern in solids. What is actually observed is a set of very sharp and well separated lines in a pattern for which the naive expectation looks like an envelope. As shown by Nacher *et al.*, this set of sharp lines is predicted whenever one takes into account the dipolar couplings between slices along the capillary. Semiquantitative agreement with experiments is even obtained with such simplistic models as a regular necklace of 48 equal classical spins, in the shape of a U or a circle, with dipolar couplings between first neighbors or between all spins. The first aim of the present paper is to indicate that a similar mechanism of spectral clustering (for small pulses) is also operative in standard high-resolution NMR in liquids, whenever the maximum equilibrium dipolar field is comparable to, or larger than, the external field inhomogeneity over the sample: The observed spectrum of the concentrated spins no longer simply reflects the distribution of external field and dipolar field. This effect will be illustrated here on a simple discrete model involving eight equal classical spins at the corners of a cube. Of course, actual observation of these dipolar field effects requires that they are not swamped by relaxation or by radiation damping [13–15]. Spectral clustering is very different from other surprising dynamical effects of the dipolar field which have been studied by Desvaux and Goldman [16] on two-line spectra in homogeneous situations.

In the course of their experiments, Nacher and Stoltz [17] also noticed that the response to large pulses (tipping angle of 0.5 rad or more) died out much more rapidly than

 0031-9007/99/82(8)/1772(4)$15.00

for "small" pulses (tipping angle of 0.2 rad or less). The second aim of the present paper is to indicate that this is a manifestation of a general instability generated by the dipolar field after large pulses, in which the spin magnetization evolves differently at close-by spatial locations, somewhat like in turbulence. Two models will be used here to examine this instability in the context of standard high resolution NMR in liquids: one involving eight equal classical spins at the corners of a cube, and one dealing with a continuous distribution of spin magnetization in a sphere. Both models predict instability for tipping angles above a threshold of the order of $\pi/4$, and rates of growth of the order of the angular velocity of the spins in the typical dipolar field created by the equilibrium magnetization. Again, observation of these effects in a standard liquid NMR experiment will require long relaxation times and efficient control of radiation damping.

In this first round of discussion of spectral clustering and instabilities, it will be convenient to examine situations in which a uniform spin magnetization in the sample (and zero outside) remains uniform, provided that all external fields are also uniform. This requires the dipolar field to be zero at all points in the sample for a uniform magnetization. Examples of such situations are provided by a spherical sample and by the model of eight equal classical spins at the corners of a cube, with dipolar coupling between first neighbors only.

For this last model, neglecting relaxation, flow, and atomic diffusion, the equation of motion for the magnetic moment $\boldsymbol{M}_j$ of the classical spin j is

$$\frac{d}{dt}\,\boldsymbol{M}_j(t) = \boldsymbol{M}_j(t) \times \gamma[\boldsymbol{B}_0 + \boldsymbol{B}_{\mathrm{inh},j} + \boldsymbol{B}_{\mathrm{dip},j}(t)], \quad (1)$$

where $\boldsymbol{B}_{\mathrm{inh},j}$ is the (small) deviation of the external magnetic field at position j from the average value $\boldsymbol{B}_0$, and the dipolar field $\boldsymbol{B}_{\mathrm{dip},j}(t)$ at position j is given by

$$\boldsymbol{B}_{\mathrm{dip},j}(t) = \sum_{g\,\mathrm{f.n.}\,j} \frac{\mu_0}{4\pi (r_{gj})^3}\,\{3[\boldsymbol{M}_g(t)\cdot\hat{\boldsymbol{r}}_{gj}]\hat{\boldsymbol{r}}_{gj} - \boldsymbol{M}_g(t)\}, \quad (2)$$

where f.n. stands for "first neighbors," $\boldsymbol{r}_{gj}$ is the vector pointing from g to j, and a caret indicates a unit vector. For $|\boldsymbol{B}_{\mathrm{dip},j}(t)|$ and $|\boldsymbol{B}_{\mathrm{inh},j}|$ very small compared to $|\boldsymbol{B}_0|$, it is convenient to use a frame of reference rotating at the angular velocity $-\gamma\boldsymbol{B}_0$ [time derivatives denoted $(d/dt)_{\mathrm{rot}}$], and terms which are not secular with respect to this rotation can be ignored to a good approximation, leading to the equations of motion

$$\left(\frac{d}{dt}\right)_{\mathrm{rot}} \boldsymbol{M}_j(t) = \boldsymbol{M}_j(t) \times \left(\gamma(\boldsymbol{B}_{\mathrm{inh},j})_z + \sum_{g\,\mathrm{f.n.}\,j} k[1 - 3(\hat{\boldsymbol{r}}_{gj})_z^2]\{\boldsymbol{M}_g(t) - 3[\boldsymbol{M}_g(t)]_z\hat{\boldsymbol{z}}\}\right), \quad (3)$$

where the z axis points in the direction of $\boldsymbol{B}_0$, and $k = \gamma\mu_0/8\pi a^3$, where a is the side of the cube. Because of the presence of the dipolar field, Eqs. (1) and (3) are sets of *nonlinear* differential equations for the components of the magnetic moments $\boldsymbol{M}_g(t)$. In "thermal equilibrium," all magnetic moments have the same value $\boldsymbol{M}_0$ which is parallel to $\boldsymbol{B}_0$.

For small deviations from thermal equilibrium, Eq. (3) can be linearized (to a first approximation), and the 24 corresponding eigenvectors and eigenvalues can be obtained numerically. The z projection of the total magnetic moment is an exact invariant of the motion (in all cases); hence, the eight eigenvectors which describe deviations of the z projection of each individual spin have eigenfrequencies of zero. The other eigenvectors describe components of the total magnetization which rotate in the xy plane at eight (different) angular velocities, with two complex conjugate eigenvectors and eigenvalues for each angular velocity to satisfy the reality condition for each $\boldsymbol{M}_j(t)$. The intensity of the absorption line at each angular velocity is proportional to the square of the modulus of the scalar product of the x projection of the total spin magnetic moment with the corresponding normalized eigenvector. Figure 1 shows the typical result of such a calculation performed as a function of the "magnitude" kM_0 of the dipolar field, for one particular set of randomly chosen deviations $\boldsymbol{B}_{\mathrm{inh},j}$ of the external field at each spin from $\boldsymbol{B}_0$. In similar models involving up to 32 spins to mimic a sample with a weak field gradient, the number of strong absorption lines progressively decreases to one or two for increasing dipolar coupling. For increasing tipping angle, numerical simulations indicate that spectral clustering persists until instability sets in.

The linear stability analysis of the above model of eight classical spins is easily performed after a pulse of arbitrary tipping angle θ applied to the thermal equilibrium state, provided that the external field is perfectly homogeneous. Indeed, in this case, the magnetic moments of the eight spins remain fixed in the rotating frame if they are all equal and parallel to each other. The results indicate that the expected synchronous free precession of all spins is dynamically stable for small tipping angles [θ between 0 and $(\pi/2 - \theta_{\mathrm{magic}})$ and between $(\pi/2 + \theta_{\mathrm{magic}})$ and π] and unstable for large tipping angles [θ between $(\pi/2 - \theta_{\mathrm{magic}})$ and $(\pi/2 + \theta_{\mathrm{magic}})$], where $\cos^2\theta_{\mathrm{magic}} = \frac{1}{3}$. For large tipping angles, numerical solutions with very small (random) initial deviations of the directions of the individual spin magnetic moments from homogeneity show the expected exponential increase of the rms deviations (at the rate predicted by the linear stability analysis) followed by turbulent motion and a strong decrease in the total precessing magnetization when the deviations have become large. Numerical solutions also show the absence of instability for small tipping angles, and indicate that the pattern of

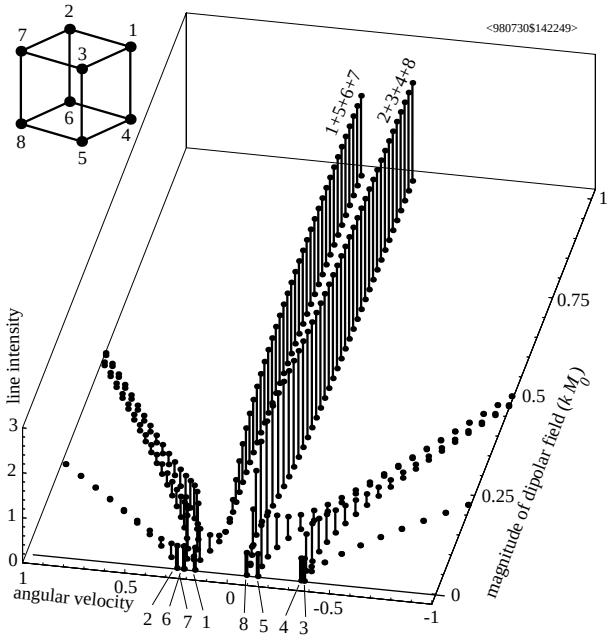

FIG. 1. The model consists in eight classical spins at the corners of a cube, in a large external magnetic field (parallel to 1,4) with small inhomogeneities. Starting from thermal equilibrium, a small pulse is applied. The Fourier transform of the response is a set of eight sharp lines, the intensities of which are shown as the vertical coordinate, as a function of the frequency ("angular velocity") and of the magnitude of the dipolar coupling between first neighbor spins ("dipolar field"). The spin(s) contributing to each line are shown for zero dipolar coupling (one line for each spin), and for the two strong lines which dominate the spectrum for large dipolar couplings. The frequency separation between these two lines is the difference between the average frequencies of spins 1,5,6,7 and 2,3,4,8 at zero dipolar field. The unexpected feature of spectral clustering is the transformation of an eight-line spectrum without dipolar coupling into an essentially two-line spectrum for large coupling.

stability and instability just described withstands the presence of inhomogeneities in the external field of the order of the dipolar coupling between spins.

A preliminary exploration of the issue of stability on various similar models of coupled classical spins (involving up to 96 spins) indicated that instabilities do not show up whenever all spins lie in a plane, and always appear (at least for tipping angles close to $\pi/2$) when they do not. For instance, in simulations of the experiments of Nacher *et al.* [17], the observed instabilities could be reproduced with a model in the shape of a necklace with "pearls" consisting of small cubes with equal classical spins at the corners, not with pearls consisting in a single classical spin. Spectral clustering, on the other hand, seems to happen in all cases.

The models using a small set of equal classical spins are obviously very rough caricatures of the actual situation in NMR experiments performed on real liquid samples. More satisfactory models would describe the spin situation in terms of the (average) magnetization $\boldsymbol{M}(\boldsymbol{r},t)$ at position $\boldsymbol{r}$ and time t (i.e., average magnetic moment per unit volume). Ignoring again relaxation and flow, the equation of motion analogous to Eq. (1) is

$$\frac{d}{dt}\boldsymbol{M}(\boldsymbol{r},t) = \boldsymbol{M}(\boldsymbol{r},t) \times \gamma[\boldsymbol{B}_0 + \boldsymbol{B}_{\rm inh}(\boldsymbol{r}) + \boldsymbol{B}_{\rm dip}(\boldsymbol{r},t)] + D\nabla^2\boldsymbol{M}(\boldsymbol{r},t), \quad (4)$$

where D is the coefficient of atomic diffusion, and the dipolar field $\boldsymbol{B}_{\rm dip}(\boldsymbol{r},t)$ at position $\boldsymbol{r}$ depends upon the distribution of the magnetization $\boldsymbol{M}(\boldsymbol{r}',t)$ over the whole sample. A simple case for this dependence is that of an infinite sample with a spatially periodic distribution of magnetization $\boldsymbol{M}_{\boldsymbol{q}}(\boldsymbol{r}) = \boldsymbol{m}_{\boldsymbol{q}}\exp(i\boldsymbol{q}\cdot\boldsymbol{r})$, where $\boldsymbol{q}$ is a (real) wave vector and $\boldsymbol{m}_{\boldsymbol{q}} = (\boldsymbol{m}_{-\boldsymbol{q}})^*$ to satisfy the reality condition for $\boldsymbol{M}(\boldsymbol{r})$. This distribution of magnetization $\boldsymbol{M}_{\boldsymbol{q}}(\boldsymbol{r})$ generates a dipolar field given by the simple expression [1,2],

$$\boldsymbol{B}_{{\rm dip},\boldsymbol{q}}(\boldsymbol{r}) = \mu_0\left\{\frac{1}{3}\boldsymbol{M}_{\boldsymbol{q}}(\boldsymbol{r}) - [\boldsymbol{M}_{\boldsymbol{q}}(\boldsymbol{r})\cdot\hat{\boldsymbol{q}}]\hat{\boldsymbol{q}}\right\}, \quad (5)$$

in which the collective origin of the dipolar field is not explicit any more, although it is still present, of course. Great care must be taken in using Eq. (5) in the context of a sample of finite size because of the long range of the dipolar interaction. For large vectors $\boldsymbol{q}$, for which the spatial wavelength $2\pi/|q|$ is much shorter than the size of the sample, Eq. (5) remains a good approximation for the positions $\boldsymbol{r}$ inside the sample at distances from the surface (much) larger than $2\pi/|q|$. However, the use of Eq. (5) precludes investigation of inhomogeneities over the length scale of the sample, and poses a problem with the components at $\boldsymbol{q} = 0$ describing the total magnetic moment [2,18]. In the present discussion, this effect of the total magnetization will be ignored by assuming a spherical sample, and reference will be given to the model with eight classical spins (discussed previously) for the behavior of inhomogeneities of the same length scale as the sample.

With these restrictions and precautions in mind, the magnetization can be expressed as a spatial Fourier series (perhaps with periodic boundary conditions over a cube surrounding the sphere)

$$\boldsymbol{M}(\boldsymbol{r},t) = \boldsymbol{M}_{\rm av}(t) + \sum_{\boldsymbol{q}\neq 0}\boldsymbol{m}_{\boldsymbol{q}}(t)e^{i\boldsymbol{q}\cdot\boldsymbol{r}}, \quad (6)$$

where $\boldsymbol{M}_{\rm av}(t)$ is the average magnetization of the sample, and the analogous of Eq. (3), for $\boldsymbol{B}_{\rm inh}(\boldsymbol{r}) = 0$, is

$$\left(\frac{d}{dt}\right)_{\rm rot}\boldsymbol{M}(\boldsymbol{r},t) = \sum_{\boldsymbol{q}}\left[\left(\boldsymbol{M}(\boldsymbol{r},t)\times\gamma\mu_0[1-3(\hat{\boldsymbol{q}}\cdot\hat{\boldsymbol{z}})^2]e^{i\boldsymbol{q}\cdot\boldsymbol{r}}\left\{\frac{1}{2}[\boldsymbol{m}_{\boldsymbol{q}}(t)\cdot\hat{\boldsymbol{z}}]\hat{\boldsymbol{z}} - \frac{1}{6}\boldsymbol{m}_{\boldsymbol{q}}(t)\right\}\right) - Dq^2\boldsymbol{m}_{\boldsymbol{q}}(t)\right]. \quad (7)$$

As a first step in the discussion of linear stability after a pulse applied to the uniform situation at thermal equilibrium, Eq. (6) is substituted into Eq. (7), and only the terms of first order in the small quantities $\boldsymbol{m}_{\boldsymbol{q}}(t)$ are retained. The only position dependences left are then a single factor $\exp(i\boldsymbol{q}\cdot\boldsymbol{r})$ in the summation over $\boldsymbol{q}$ in the left-hand side, and a similar single factor $\exp(i\boldsymbol{q}'\cdot\boldsymbol{r})$ in the summation over $\boldsymbol{q}'$ in the right-hand side of the expression; hence, a single equality results for each separate wave vector $\boldsymbol{q}$,

$$\left(\frac{d}{dt}\right)_{\text{rot}} \boldsymbol{m}_{\boldsymbol{q}}(t) = \boldsymbol{M}_{\text{av}}(t) \times \gamma\mu_0([1 - 3(\hat{\boldsymbol{q}}\cdot\hat{z})^2]\{\tfrac{1}{2}[\boldsymbol{m}_{\boldsymbol{q}}(t)\cdot\hat{z}]\hat{z} - \tfrac{1}{6}\boldsymbol{m}_{\boldsymbol{q}}(t)\}) - Dq^2\boldsymbol{m}_{\boldsymbol{q}}(t)\,, \tag{8}$$

where $\boldsymbol{M}_{\text{av}}$ is immobile with respect to the rotating frame. Note that this immobility lasts only as long as the inhomogeneities remain very small. For each wave vector $\boldsymbol{q}$, Eq. (8) has three eigenvectors $\boldsymbol{m}_{\boldsymbol{q},s}(t)$ and eigenvalues $\upsilon_{\boldsymbol{q},s}$, such that $\boldsymbol{m}_{\boldsymbol{q},s}(t) = \boldsymbol{m}_{\boldsymbol{q},s}(0)\exp(\upsilon_{\boldsymbol{q},s}t)$. Figure 2 shows the dependence of the real part of these eigenvalues upon the tipping angle from equilibrium and the coefficient of atomic diffusion. For $D = 0$, positive eigenvalues, hence, instabilities, appear in the same range of large tipping angles as for the model with eight classical spins discussed above. Increasing Dq^2 decreases this range down to zero width.

In the case of liquid water in equilibrium at 298 K, at a proton NMR frequency of 600 MHz, for $\boldsymbol{q}$ parallel to the external field, for a tipping angle $\theta = \pi/2$, and ignoring relaxation, the rate of growth of the unstable modes is about 7.2 s^{-1} for long wavelengths (negligible Dq^2), and diffusion suppresses the instabilities for wavelengths shorter than about 0.11 mm. For the discrete model with eight spins, taking M_0/a^3 as the magnetization, the corresponding maximum rate of growth is 3.3 s^{-1}.

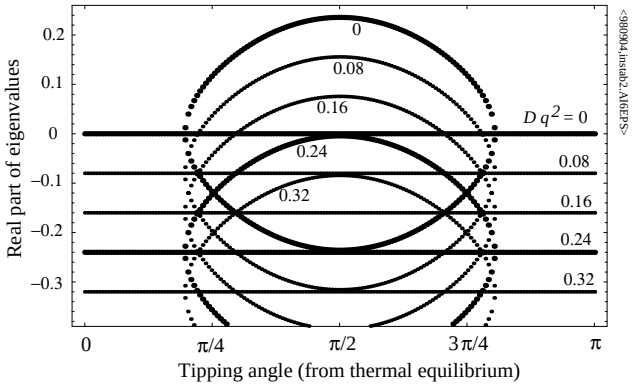

FIG. 2. The model consists in a continuous distribution of spin magnetization, with deviations from uniformity described as a superposition of harmonic plane waves with wave vectors $\boldsymbol{q}$. Starting from equilibrium, all magnetization is tipped by the angle θ, resulting in a uniform precessing magnetization $\boldsymbol{M}_{\text{av}}$. The linear stability analysis of this situation leads to eigenvalues which are shown here as a function of θ for a number of values of the atomic diffusion constant D. The behavior of the corresponding modes is governed by the real part of the eigenvalues: unstable modes for positive real parts, undamped oscillations for zero real parts, and damped motion for negative real parts. These real parts and Dq^2 are shown here in units of $|M_{\text{av}}\gamma\mu_0[1 - 3(\hat{\boldsymbol{q}}\cdot\hat{\boldsymbol{z}})^2]|$.

All of this indicates that spectral clustering for small tipping angles and dynamical instability for large tipping angles (the usual situation in most experiments) is a very general feature of magnetic resonance of concentrated spin systems in liquids. Presumably, instability and clustering will show up in standard high resolution NMR experiments as soon as the spectrometers will be provided with efficient means of suppressing strong radiation damping. Let us stress that the effects discussed here are macroscopic classical phenomena related to spatial inhomogeneities, which do not require a detailed quantum description for their interpretation.

Illuminating discussions with Pierre-Jean Nacher and Eric Stoltz are gratefully acknowledged.

*Email address: jjeener@ulb.ac.be

[1] G. Deville, M. Bernier, and J. M. Delrieux, Phys. Rev. B **19**, 5666 (1979).
[2] A. Abragam and M. Goldman, *Nuclear Magnetism: Order and Disorder* (Clarendon Press, Oxford, 1982).
[3] H. T. Edzes, J. Magn. Reson. **86**, 293 (1990).
[4] R. Bowtell, R. M. Bowley, and P. Glover, J. Magn. Reson. **88**, 643 (1990).
[5] Q. He, W. Richter, S. Vathyam, and W. S. Warren, J. Chem. Phys. **98**, 6779 (1993).
[6] W. S. Warren, W. Richter, A. H. Andreotti, and B. T. Farmer II, Science **262**, 2005 (1993).
[7] J. Jeener, A. Vlassenbroek, and P. Broekaert, J. Chem. Phys. **103**, 1309 (1995).
[8] M. H. Levitt, Concepts Magn. Reson. **8**, 77 (1996).
[9] A. Vlassenbroek, J. Jeener, and P. Broekaert, J. Magn. Reson. A **118**, 234 (1996).
[10] D. Candela, M. E. Hayden, and P.-J. Nacher, Phys. Rev. Lett. **73**, 2587 (1994).
[11] E. Stoltz, J. Tannenhauser, and P.-J. Nacher, J. Low Temp. Phys. A **101**, 839 (1995).
[12] E. Stoltz, Ph.D. thesis, Université Paris 6, 1996.
[13] N. Bloembergen and R. V. Pound, Phys. Rev. **95**, 8 (1954).
[14] C. R. Bruce, R. E. Norberg, and G. E. Pake, Phys. Rev. **104**, 419 (1956).
[15] P. Broekaert and J. Jeener, J. Magn. Reson. A **113**, 60 (1995).
[16] M. Goldman and H. Desvaux, Chem. Phys. Lett. **256**, 497 (1996).
[17] P.-J. Nacher and E. Stoltz (private communication).
[18] W. S. Warren, S. Lee, W. Richter, and S. Vathyam, Chem. Phys. Lett. **247**, 207 (1995).